

Synthesis and characterization of $[\text{Fe}(\text{III})(\text{qsal})_2][\text{M}(\text{III})(\text{pds})_2]$ ($\text{M} = \text{Cu}, \text{Au}$)

J.C. Dias^{*}, A. Soriano-Portillo, M. Clemente-Léon, C. Giménez-Saiz, J.R. Galán-Mascarós,
C.J. Gómez-García, E. Coronado

Instituto de Ciencia Molecular (ICMol), Universidad de Valencia, Polígono de la Coma s/n, E-46980 Paterna, Spain

Received 4 December 2006; accepted 9 February 2007

Available online 15 February 2007

Paper presented in the MAGMANet-ECMM, European Conference on Molecular Magnetism.

Abstract

Salts of the Fe(III) spin crossover cation $[\text{Fe}^{\text{III}}(\text{qsal})_2]^+$ ($\text{qsalH} = N$ -(8-quinolyl)salicylalimine) and monoanions $[\text{M}^{\text{III}}(\text{pds})_2]^-$ ($\text{M} = \text{Cu}, \text{Au}$; $\text{pds} = \text{pirazine-2,3-diselenolate}$) with formula $[\text{Fe}^{\text{III}}(\text{qsal})_2][\text{M}^{\text{III}}(\text{pds})_2]$ were prepared and characterized by single crystal X-ray diffraction and magnetic measurements. These two salts present magnetic properties essentially due to the Fe^{III} centres in the high-spin state ($S = 5/2$), and do not have any spin transition.

© 2007 Elsevier B.V. All rights reserved.

Keywords: Spin crossover; Magnetic properties

1. Introduction

Spin crossover is a phenomenon in which the variation in temperature, pressure or the light irradiation may lead to a spin transition, from the low-spin (LS) state to the high-spin (HS) state or vice versa. This transition is indicated by a magnetic and structural change, and depends strongly on the cooperativity between building blocks. Although Fe(II) are the most common spin crossover compounds, however, a few Fe(III) complexes can be compared to these. In fact, the first spin crossover compound discovered was of Fe(III) [1]. Thus, $[\text{Fe}^{\text{III}}(\text{qsal})_2]^+$ ($\text{qsalH} = N$ -(8-quinolyl)salicylalimine) is a cation able to exhibit spin crossover properties: $[\text{Fe}^{\text{III}}(\text{qsal})_2](\text{NCS})$ [2] presents this kind of transition. However, spin crossover is a counter-ion-dependent phenomenon, e.g., for $[\text{Fe}^{\text{III}}(\text{qsal})_2](\text{NCS})$ the transition has a more gradual character,

with hysteresis, than for $[\text{Fe}^{\text{III}}(\text{qsal})_2](\text{NCSe}) \cdot \text{CH}_2\text{Cl}_2$ [3], where the transition has an abrupt character with a very wide hysteresis: the reason is the cooperative interaction.

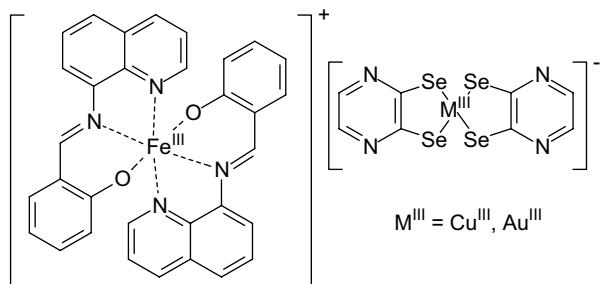
Aiming at obtaining spin crossover salts, we synthesize and characterize new salts with this cation and planar bis(dichalcogenolate)metalate(III) complexes as anions: $[\text{Cu}^{\text{III}}(\text{pds})_2]^-$ and $[\text{Au}^{\text{III}}(\text{pds})_2]^-$ ($\text{pds} = \text{pirazine-2,3-diselenolate}$). Scheme 1 shows the building blocks and the compounds synthesized: $[\text{Fe}^{\text{III}}(\text{qsal})_2][\text{Cu}^{\text{III}}(\text{pds})_2]$ (1) and $[\text{Fe}^{\text{III}}(\text{qsal})_2][\text{Au}^{\text{III}}(\text{pds})_2]$ (2).

2. Experimental

2.1. Synthesis

Compound $[\text{Fe}^{\text{III}}(\text{qsal})_2]\text{Cl} \cdot 1.5\text{H}_2\text{O}$ was synthesized according to the method of Ref. [2]. $(n\text{-Bu}_4\text{N})[\text{Cu}^{\text{III}}(\text{pds})_2]$ [4] and $(n\text{-Bu}_4\text{N})[\text{Au}^{\text{III}}(\text{pds})_2]$ [5] were synthesized according to the literature procedures. The solvents were used without further purification.

^{*} Corresponding author. Tel.: +34 96 354 44 24; fax: +34 96 354 32 73.
E-mail address: joao.dias@uv.es (J.C. Dias).



Scheme 1.

$[\text{Fe}^{\text{III}}(\text{qsal})_2][\text{Cu}^{\text{III}}(\text{pds})_2]$ (**1**) and $[\text{Fe}^{\text{III}}(\text{qsal})_2][\text{Au}^{\text{III}}(\text{pds})_2]$ (**2**) were prepared by slow diffusion of a solution of $[\text{Fe}^{\text{III}}(\text{qsal})_2]\text{Cl} \cdot 1.5\text{H}_2\text{O}$ in a solution of $(n\text{-Bu}_4\text{N})[\text{Cu}^{\text{III}}(\text{pds})_2]$ or $(n\text{-Bu}_4\text{N})[\text{Au}^{\text{III}}(\text{pds})_2]$, respectively, in acetonitrile.

2.2. X-ray crystallography

The crystal structures of compounds **1** and **2** were determined from single crystal X-ray diffraction data collected at 295(2) K for **1** and at 180(2) K for **2**. Data were collected with a Nonius Kappa CCD diffractometer using a graphite monochromated Mo $K\alpha$ radiation source ($\lambda = 0.71073 \text{ \AA}$).

Denzo and Scalepack [6] programs were used for cell refinements and data reduction. The structures were solved by direct methods using the SIR97 [7] program with the WINGX [8] graphical user interface. The structure refinements were carried out with SHELX-97 [9]. A multiscan absorption correction, based on equivalent reflections, was applied to the data using the program SORTAV [10]. All nonhydrogen atoms were refined anisotropically. Hydrogen atoms on carbon atoms were included at calculated positions and refined with a riding model. Crystal data are tabulated in Table 1.

2.3. Magnetic measurements

Variable temperature susceptibility measurements were carried out in the temperature range 2–300 K at an applied magnetic field of 0.1 T on polycrystalline samples of compounds **1** and **2** with a Quantum Design MPMS-XL-5 SQUID magnetometer. Isothermal magnetizations were performed at 2 K with magnetic fields between 0 and 5 T in the same SQUID magnetometer for compound **1**. The susceptibility data were corrected for the sample holder previously measured using the same conditions and for the diamagnetic contributions of the salt as deduced by using Pascal's constant tables.

Table 1
Crystal data and structural refinement of compounds **1** and **2**

	$[\text{Fe}^{\text{III}}(\text{qsal})_2][\text{Cu}^{\text{III}}(\text{pds})_2]$ (1)	$[\text{Fe}^{\text{III}}(\text{qsal})_2][\text{Au}^{\text{III}}(\text{pds})_2]$ (2)
Empirical formula	$\text{C}_{40}\text{H}_{26}\text{CuFeN}_8\text{O}_2\text{Se}_4$	$\text{C}_{40}\text{H}_{26}\text{AuFeN}_8\text{O}_2\text{Se}_4$
Formula weight	1085.92	1219.34
<i>T</i> (K)	295(2)	180(2)
Wavelength (\AA)	0.71073	0.71073
Crystal system	monoclinic	monoclinic
Space group	$P2_1/c$	$P2_1/c$
Unit cell dimensions		
<i>a</i> (\AA)	13.7715(2)	13.7634(2)
<i>b</i> (\AA)	10.7457(2)	10.65560(15)
<i>c</i> (\AA)	26.4668(3)	26.5852(5)
α ($^\circ$)	90	90
β ($^\circ$)	97.2177(5)	97.9148(5)
γ ($^\circ$)	90	90
<i>V</i> (\AA^3)	3885.64(10)	3861.77(11)
<i>Z</i>	4	4
<i>D</i> _{calc} (Mg/m^3)	1.856	2.097
μ (mm^{-1})	4.716	7.989
<i>F</i> (000)	2116	2316
Crystal size (mm)	$0.25 \times 0.20 \times 0.20$	$0.20 \times 0.15 \times 0.10$
θ Range ($^\circ$)	3.10–27.28	2.99–27.47
<i>h, k, l</i> Ranges	–17/17, –13/13, –33/33	–17/17, –13/13, –34/34
Reflections collected	16724	16516
Independent reflections [<i>R</i> _{int}]	8635 [0.0326]	8739 [0.0692]
Completeness to θ (%)	99.1	98.7
Transmission – maximum/minimum	0.394/0.338	0.455/0.242
Refinement method	full-matrix least-squares on F^2	full-matrix least-squares on F^2
Data/restraints/parameters	8635/0/505	8739/0/505
Goodness-of-fit on F^2	1.027	0.979
<i>R</i> [$I > 2\sigma(I)$]	$R_1 = 0.0400$, $wR_2 = 0.0887$	$R_1 = 0.0493$, $wR_2 = 0.0919$
<i>R</i> (all data)	$R_1 = 0.0784$, $wR_2 = 0.1002$	$R_1 = 0.1066$, $wR_2 = 0.1080$
Largest difference peak/hole (e \AA^{-3})	1.425/–0.994	0.771/–1.188

Download English Version:

<https://daneshyari.com/en/article/1310353>

Download Persian Version:

<https://daneshyari.com/article/1310353>

[Daneshyari.com](https://daneshyari.com)